

多输入多输出变量带误差模型的最坏情况频域辨识

耿立辉[†], 崔世钢, 赵 丽

(天津职业技术师范大学 自动化与电气工程学院 天津市信息传感与智能控制重点实验室, 天津 300222)

摘要: 本文将单输入单输出(SISO)变量带误差(EIV)模型的频域最坏情况辨识方法推广应用于多输入多输出(MIMO)情况. 类似于SISO情况, 多输入多输出变量带误差(MIMO EIV)模型的辨识模型集合由估计的系统名义模型及其最坏情况误差界描述. 所估计的系统名义模型表征为正规右图符号, 其最坏情况误差界具有可能的更少保守性, 可利用EIV模型的先验信息和后验信息由v-gap度量量化得到. 因此, 这种模型集合非常适合于后期利用Vinnicombe提出的 H_∞ 回路成形法设计鲁棒控制器. 最后, 利用一数值仿真实例验证所提出辨识方法的有效性.

关键词: 最坏情况辨识; 变量带误差(EIV)模型; 多输入多输出(MIMO); 频域; v-gap度量

中图分类号: N945.14 文献标识码: A

Frequency-domain worst-case identification of multiple input multiple output errors-in-variables models

GENG Li-hui[†], CUI Shi-gang, ZHAO Li

(Tianjin Key Laboratory of Information Sensing and Intelligent Control,

School of Automation and Electrical Engineering, Tianjin University of Technology and Education, Tianjin 300222, China)

Abstract: This paper extends a frequency-domain worst-case identification method for single input single output (SISO) errors-in-variables (EIV) models to its multiple input multiple output (MIMO) case. Similar to the SISO case, the identified model set for a MIMO EIV model is described by an estimated nominal system model and its worst-case error bound. The estimated nominal system model is characterized by a normalized right graph symbol and its worst-case error bound with possibly less conservativeness is quantified by the v-gap metric using a priori and a posteriori information on the EIV model. As a consequence, such model set is well suited to subsequent robust controller design via the H_∞ loop-shaping method proposed by Vinnicombe. Finally, the proposed identification method is verified by a numerical simulation example.

Key words: worst-case identification; errors-in-variables (EIV) models; multiple input multiple output (MIMO); frequency-domain; v-gap metric

1 Introduction

It is well-known that a large number of multiple input multiple output (MIMO) errors-in-variables (EIV) models exist in the real world. Take the aerospace engineering area as an example, an attitude model of a free-flying aircraft usually has 3 inputs and 3 outputs, which may be rotational torques and attitude angles in the body coordinate axes, respectively. However, the available measurements for these variables are typically superimposed by various disturbing noises and thus result in a MIMO EIV model. As a consequence, investigations on identification methods for such models have particularly significant application values.

Generally speaking, MIMO EIV model identification methods can be classified into two major categories. One category is capable of providing users with

a nominal system model and a possible noise model. Such models usually have uniqueness, i.e., identifiability, and the corresponding methods mainly derive from classical parameter identification methods^[1-2]. The other category can supply users a model set, which consists of numerous models and thus there exists no uniqueness. Söderström put forward a very general estimation method for the identification of system and noise models in terms of construction of instrumental variables^[3]. A recursive identification method for estimating matrix coefficients of the multivariable EIV systems was investigated by Chen^[4]. Guidorzi and Diversi proposed a Frisch scheme based EIV identification method when inputs and outputs are corrupted with white noises^[5-6]. On the basis of a consensus algorithm, Stanković et al. studied a decentralized identification approach for the

Received 1 December 2015; accepted 28 June 2016.

[†]Corresponding author. E-mail: glh2010@tute.edu.cn; Tel.: +86 13512240510.

Recommended by Associate Editor: SUN Zhendong.

Supported by National Natural Science Foundation of China (61203119, 61304153), Key Program of Tianjin Natural Science Foundation, China (14JCZDJC36300) and Tianjin University of Technology and Education Funded Project (RC14-48).

MIMO EIV models^[7]. Subspace state-space identification (4SID) methods are also available for MIMO EIV model identification^[8]. Although the state-space realizations given by the 4SID methods are non-unique, their representations in the form of transfer functions are the same. Apart from the aforementioned identification methods belonging to the first category, the second category also has undergone great developments. Green and Anderson contributed a frequency-domain estimation method dealing with MIMO EIV model^[9]. Roorda and Heij presented the global total least-squares algorithm to estimate time-domain multivariable EIV models^[10]. Under some certain deterministic framework, Geng et al. extended a frequency-domain L_2 -optimal identification method to the MIMO case and studied its algorithm implementation issues^[11-12].

The major contribution of this paper is to extend an original worst-case identification method for (SISO EIV) models to its MIMO case. Similar to the SISO case, the identified model set is comprised of a nominal system model and its worst-case error bound. In order to quantify a less conservative worst-case error bound for the MIMO nominal system model, the v-gap metric is employed as not only a minimization criterion for parameter estimation but also a metric for characterization of input and output disturbing noises^[13-14]. However, the quantification of the worst-case error in the MIMO framework is more difficult than that in the SISO case and thus needs more investigations. As a consequence, this paper first proposes an underlying MIMO EIV identification framework. Then, a new quantification method is derived to determine the worst-case error bound for a nominal system model optimized from the minimization of the v-gap metric criterion. With this error bound in hand, the convergent theorem for the identification algorithm can be obtained subsequently. The most charming feature of the proposed method is that an advanced loop-shaping based robust controller design approach is readily available for such model set^[15]. This kind of model set makes sharp comparison with the resulting models obtained from the most existing EIV model identification methods since the controller synthesis for the latter models needs further research in the future.

The notations in this paper are stated as follows. \mathcal{T} represents the set of angular frequencies in the interval $[0, 2\pi]$. $L_2^{m \times n}$, $L_\infty^{m \times n}$, $H_2^{m \times n}$ and $H_\infty^{m \times n}$ are the function subspaces in the Hardy space. $\delta_v(M_1, M_2)$ denotes the v-gap metric of $M_1(\lambda) \in H_\infty^{p \times q}$ and $M_2(\lambda) \in H_\infty^{p \times q}$. $\bar{\sigma}(X)$ and $\underline{\sigma}(X)$ represent the maximum and minimum singular values of the complex matrix X , respectively. For any $M(\lambda) \in L_\infty^{p \times q}$, $M^*(\lambda) = M^T(\lambda^{-1})$. $\mathbb{C}^{m \times n}$ stands for the subspace of $m \times n$ -dimensional complex matrices. $\mathbb{R}^{m \times n}$ stands for the subspace of $m \times n$ -dimensional real matrices.

The remainder of this paper is organized as follows. Section 2 formulates an underlying MIMO EIV identification framework. In Section 3, the quantification of the worst-case error for the nominal system model and the derivation of the robust convergent theorem are detailed. Both constraint conditions and implementation steps for the identification algorithm are addressed in Section 4. Section 5 uses a numerical simulation to demonstrate the effectiveness of the proposed method. Finally, conclusions related to this study are drawn in Section 6.

2 Problem formulation

The paper considers the MIMO EIV model structure shown in Fig.1, in which the following deterministic signal relations hold

$$y(\lambda) = P_0(\lambda)u(\lambda), \tag{1}$$

$$\begin{bmatrix} y_m(\lambda) \\ u_m(\lambda) \end{bmatrix} = \begin{bmatrix} y(\lambda) \\ u(\lambda) \end{bmatrix} + \begin{bmatrix} n_y(\lambda) \\ n_u(\lambda) \end{bmatrix}, \tag{2}$$

where $P_0(\lambda) \in H_\infty^{p \times q}$ is an open-loop MIMO discrete-time time-invariant linear “true” system; $u(\lambda) = [u_1(\lambda) \cdots u_q(\lambda)]^T \in L_2^q$ and $y(\lambda) = [y_1(\lambda) \cdots y_p(\lambda)]^T \in L_2^p$ are q -dimensional input variable and p -dimensional output variable, respectively; the additive superimposition of the input noise $n_u(\lambda) = [n_u^1(\lambda) \cdots n_u^q(\lambda)]^T \in L_2^q$ and the output noise $n_y(\lambda) = [n_y^1(\lambda) \cdots n_y^p(\lambda)]^T \in L_2^p$ on $u(\lambda)$ and $y(\lambda)$ results in the measurable input variable $u_m(\lambda) = [u_m^1(\lambda) \cdots u_m^q(\lambda)]^T \in L_2^q$ and the measurable output variable $y_m(\lambda) = [y_m^1(\lambda) \cdots y_m^p(\lambda)]^T \in L_2^p$, respectively. The following assumption is made for the identification of the MIMO EIV model in Fig.1.

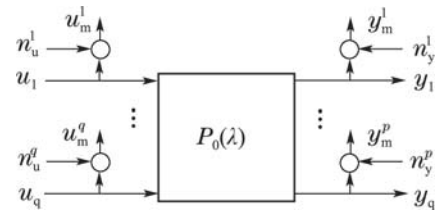


Fig. 1 An MIMO EIV model structure

Assumption 1 The disturbing noises n_y and n_u belong to the following noise set:

$$\mathcal{S}_{N_1}(\epsilon, \rho_0) \triangleq \{(n_y, n_u) : \delta_v(P_0, P_m) \leq \epsilon < \rho_0, \rho_0 \triangleq \inf_{\omega \in \mathcal{T}} \underline{\sigma}(D_0(e^{j\omega}))\}, \tag{3}$$

where

$$P_m(\lambda) \triangleq \begin{bmatrix} \frac{y_m^1(\lambda)}{u_m^1(\lambda)} & \cdots & \frac{y_m^1(\lambda)}{u_m^q(\lambda)} \\ \vdots & \ddots & \vdots \\ \frac{y_m^p(\lambda)}{u_m^1(\lambda)} & \cdots & \frac{y_m^p(\lambda)}{u_m^q(\lambda)} \end{bmatrix} \in L_\infty^{p \times q}, \tag{4}$$

$D_0(e^{j\omega})$ is the frequency response of the denominator factor of a normalized right graph symbol (NRGS)

$G_0(\lambda) = [N_0^T(\lambda) \ D_0^T(\lambda)]^T \in \mathbb{H}_\infty^{(p+q) \times q}$ of $P_0(\lambda)$.

The above assumption is in part used to ensure that the disturbed model $P_m(\lambda)$ defined in (4) belongs to $\mathbb{H}_\infty^{p \times q}$ and suppose that $G_m(\lambda) = [N_m^T(\lambda) \ D_m^T(\lambda)]^T \in \mathbb{H}_\infty^{(p+q) \times q}$ is one of its NRGs.

The a priori model set of the open-loop system $P_0(\lambda)$ can be defined by its NRGs in the following way:

$$\mathcal{S}_{\mathcal{M}}(\beta) \triangleq \{G_P(\lambda) : \|\dot{G}_P\|_\infty \leq \beta, \\ G_P(\lambda) \in \mathcal{S}_{\mathcal{G}}(P_0)\}, \quad (5)$$

where \dot{G}_P denotes the first-order derivative of $G_P(\lambda)$ with respect to λ and $\mathcal{S}_{\mathcal{G}}(P_0)$ is the NRGs set of $P_0(\lambda)$. The models belonging to $\mathcal{S}_{\mathcal{M}}(\beta)$ are thus implied to be continuous with respect to λ .

The available a posteriori frequency-domain experimental data collected from identification experiments are defined as

$$\mathcal{S}_{\mathcal{D}}(\mathcal{W}) \triangleq \{(y_m^{\omega_i}, u_m^{\omega_i}) \triangleq (y_m(e^{j\omega_i}), u_m(e^{j\omega_i})) : \\ \omega_i \in \mathcal{W} \triangleq \{\omega_1, \dots, \omega_N\} \text{ and} \\ \omega_1 < \omega_2 < \dots < \omega_N\} \quad (6)$$

with N being the length of sampled data. Since a Nyquist plot of any discrete-time transfer function has the symmetry with respect to the real axis, it is sufficient to use the sampling angular frequencies in an interval $(0, \pi)$ for the identification. The maximum gap between the adjacent angular frequencies in \mathcal{W} is thus computed as

$$\bar{\delta} \triangleq \max\{\omega_1, \pi - \omega_N, \max_{i \in \mathcal{N}}\{\omega_{i+1} - \omega_i\}\} \quad (7)$$

with $\mathcal{N} \triangleq \{1, \dots, N-1\}$.

In the foregoing stated MIMO EIV framework, the identification objectives are two folds (i) use the a posteriori frequency-domain measurements $\mathcal{S}_{\mathcal{D}}(\mathcal{W})$ from the angular frequency interval $(0, \pi)$ to estimate a nominal system model $P(\lambda) \in \mathbb{H}_\infty^{p \times q}$ with $G(\lambda) \in \mathbb{H}_\infty^{(p+q) \times q}$ being one of its NRGs and (ii) quantify the worst-case error of $P(\lambda)$ as an upper bound τ according to the a priori sets $\mathcal{S}_{\mathcal{N}_1}(\epsilon, \rho_0)$ and $\mathcal{S}_{\mathcal{M}}(\beta)$. As a result, $P(\lambda)$ and τ are able to describe a model set, which is well suited to the robust controller synthesis.

3 Identification algorithm

Similar to the SISO case, the following minimization criterion for estimation of the nominal model $P(\lambda)$ is employed^[13-14, 16]

$$\min_{\substack{X \in \mathbb{R}^{(p+q) \times nq} \\ Q_F^{\omega_i} \in \mathbb{C}^{q \times q}}} \max_{\omega_i \in \mathcal{W}} \{\bar{\sigma}(G_m^{\omega_i} - F_X^{\omega_i} Q_F^{\omega_i})\}, \\ c \|\dot{F}_X\|_\infty\}, \quad (8)$$

where $G_m^{\omega_i}$ is the frequency response of $G_m(\lambda)$ evaluated at $\omega_i \in \mathcal{W}$ and can be generated by

$$G_m^{\omega_i} = \begin{bmatrix} N_m^{\omega_i} \\ D_m^{\omega_i} \end{bmatrix} \triangleq G_m(e^{j\omega_i}) = \begin{bmatrix} N_m(e^{j\omega_i}) \\ D_m(e^{j\omega_i}) \end{bmatrix} = \\ \begin{bmatrix} P_m^{\omega_i} [I_q + (P_m^{\omega_i})^* P_m^{\omega_i}]^{-\frac{1}{2}} \\ [I_q + (P_m^{\omega_i})^* P_m^{\omega_i}]^{-\frac{1}{2}} \end{bmatrix} \quad (9)$$

with $P_m^{\omega_i}$ being the frequency response of $P_m(\lambda)$ evaluated at $\omega_i \in \mathcal{W}$; $F_X^{\omega_i}$ is the frequency response of a parameterized right factor model $F_X(\lambda) = [(N_F^X(\lambda))^T \ (D_F^X(\lambda))^T]^T$ of $P(\lambda)$, i.e., $P(\lambda) = N_F^X(\lambda)(D_F^X(\lambda))^{-1}$ and it is an affine function of X

$$F_X(\lambda) = \begin{bmatrix} N_F^X(\lambda) \\ D_F^X(\lambda) \end{bmatrix} = \\ \begin{bmatrix} X_N^1 & X_N^2 & \dots & X_N^n \\ X_D^1 & X_D^2 & \dots & X_D^n \end{bmatrix} [I_q \otimes \Lambda(\lambda)] = \\ \begin{bmatrix} X_N \\ X_D \end{bmatrix} V(\lambda) = XV(\lambda), \quad (10)$$

where $\Lambda(\lambda) \triangleq [1 \ \lambda \ \dots \ \lambda^{n-1}]^T$ and \otimes stands for the Kronecker product; $Q_F^{\omega_i} \in \mathbb{C}^{q \times q}$ is a complex matrix to be optimized at ω_i ; c is a user-chosen constant weight and \dot{F}_X is the first-order derivative of $F_X(\lambda)$ with respect to λ .

It is noted that the optimization criterion in (8) minimizes two objective functions at the same time. The former one is the frequency-point-wise v-gap metric between $P_m(\lambda)$ and $P(\lambda)$ provided the associated Nyquist winding condition $\text{wno}[\det(G_m^* F)] = 0$ is satisfied, which can reduce to a constraint condition on $D_F^X(\lambda)$ by the following lemma (c.f. [13]).

Lemma 1 If $\bar{\sigma}(\tilde{G}_m G)(e^{j\omega}) < \rho_1 \triangleq \inf_{\omega \in \mathcal{T}} \underline{\sigma}(D_m(e^{j\omega}))$ holds for any $\omega \in \mathcal{T}$ where $\tilde{G}_m(e^{j\omega})$ is the frequency response of a normalized left graph symbol $\tilde{G}_m(\lambda) \in \mathbb{H}_\infty^{(p+q) \times q}$ of $P_m(\lambda)$, then $\text{wno}[\det(G_m^* F)] = 0$ is implied by the condition that $D_F^X(\lambda)$ is a unit function in $\mathbb{H}_\infty^{q \times q}$.

Proof The proof process can refer to that of Lemma 3.1 addressed in [13].

The latter objective function to be minimized in (8) is the weighted worst-case derivative of $F_X(\lambda)$, which can be used to guarantee some smoothness of $F_X(\lambda)$ and thus can reduce an overfitting effect. This optimization problem can be recursively solved by a two-step iterative procedure, in which c is selected as a function of the maximum angular frequency gap $\bar{\delta}$, i.e., $c = \tilde{c}(\bar{\delta})^r$ with $\tilde{c} \in (0, \infty)$ and $r \in (0.5, 1)^{[13-14]}$.

3.1 Error quantification

The related worst-case error for the nominal system model $\hat{P}(\lambda) \triangleq \hat{N}_F^X(\lambda)(\hat{D}_F^X(\lambda))^{-1}$ optimized from (8) is defined as follows:

$$e_{\text{wc}}(\beta, \epsilon, n, p, q, \bar{\delta}, \tilde{c}, r, h) \triangleq \\ \sup_{\substack{G_0(\lambda) \in \mathcal{S}_{\mathcal{M}}(\beta) \\ (n_y, n_u) \in \mathcal{S}_{\mathcal{N}_1}(\epsilon, \rho_0) \cap \mathcal{S}_{\mathcal{N}_2}(\rho_1, \rho_2)}} \delta_v(P_0, \hat{P}), \quad (11)$$

where h is an upper bound for the L_∞ -norm of $\hat{Q}_F(\lambda)$ whose pointwise frequency response $\hat{Q}_F^{\omega_i}$ can be optimized from (8), $\mathcal{S}_{\mathcal{N}_2}(\rho_1, \rho_2)$ is a complementary noise set to ensure the existence of $\delta_v(P_0, \hat{P})$. The definition of this noise set and the quantification of h will be addressed in Section 4.

In order to determine a worst-case error upper bound for e_{wc} , the following lemma should be first introduced.

Lemma 2 According to Assumption 1, the following frequency-domain perturbed NRGS model set holds

$$G_m(e^{j\omega}) = G_0(e^{j\omega}) + \Delta(e^{j\omega}), \sup_{\omega \in \mathcal{T}} \bar{\sigma}(\Delta(e^{j\omega})) \leq \alpha, \quad (12)$$

where $\Delta(e^{j\omega}) = [\Delta_n^T(e^{j\omega}) \quad \Delta_d^T(e^{j\omega})]^T$ is the perturbation to $G_0(e^{j\omega})$ due to the disturbing noises (n_y, n_u) and $\alpha \triangleq \sqrt{2 - 2\sqrt{1 - \epsilon^2}}$.

Proof The proof for this lemma can make reference to [13].

On the basis of Lemma 2, the following theorem can be further derived.

Theorem 1 For the a priori information $(n_y, n_u) \in \mathcal{S}_{\mathcal{N}_1}(\epsilon, \rho_0)$ as well as $G_0(\lambda) \in \mathcal{S}_{\mathcal{M}}(\beta)$ and the a posteriori frequency response information $G_m^{\omega_i}$ in (12) generated from $\mathcal{S}_{\mathcal{D}}(\mathcal{W})$, there exists an $(n - 1)$ th order polynomial matrix $\bar{F}(\lambda) = [(\bar{N}_F(\lambda))^T (\bar{D}_F(\lambda))^T]^T \in \mathbb{H}_\infty^{(p+q) \times q}$ such that for any $\omega_i \in \mathcal{W}$

$$\begin{cases} \bar{\sigma}(G_m(e^{j\omega_i}) - \bar{F}(e^{j\omega_i})) \leq \sqrt{q(p+q)}\left(\alpha + \frac{\beta}{n} + \frac{\beta\delta}{4}\right), \\ \|\dot{\bar{F}}\|_\infty < \sqrt{q(p+q)}\left(\beta + \frac{2\beta}{n\delta}\right), \end{cases} \quad (13)$$

where each of entries in $\bar{N}_F(\lambda)$ and $\bar{D}_F(\lambda)$ is spanned by $\{1, \lambda, \dots, \lambda^{n-1}\}$ and δ can be determined as $2\sqrt{\delta/n}$.

Proof From the frequency-domain perturbed model given in Lemma 2, it is known that for any $\omega_i \in \mathcal{W}$, the following pointwise frequency response equation holds

$$G_m^{(kl)}(e^{j\omega_i}) = G_0^{(kl)}(e^{j\omega_i}) + \Delta^{(kl)}(e^{j\omega_i}), \quad |\Delta^{(kl)}(e^{j\omega_i})| \leq \alpha, \quad (14)$$

where $Y^{(kl)}(e^{j\omega_i})$ denotes the entry of $Y(e^{j\omega_i})$ at the k th row and l th column with $k \in \mathcal{K} \triangleq \{1, 2, \dots, p+q\}$ and $l \in \mathcal{L} \triangleq \{1, 2, \dots, q\}$. Also note from the definition of the model set $\mathcal{S}_{\mathcal{M}}(\beta)$ in (5) that

$$\|\dot{G}_0^{(kl)}\|_\infty \leq \beta, \quad k \in \mathcal{K}, \quad l \in \mathcal{L} \quad (15)$$

with $\dot{G}_0^{(kl)}$ representing the first order derivative of the (k, l) entry in $G_0(\lambda)$ with respect to λ . In terms of (14)

and (15), there exist $q(p+q) (n-1)$ th order polynomials $\bar{F}^{(kl)}(\lambda)$, $k = 1, 2, \dots, p+q$ and $l = 1, 2, \dots, q$ such that

$$\begin{cases} |G_m^{(kl)}(e^{j\omega_i}) - \bar{F}^{(kl)}(e^{j\omega_i})| \leq \alpha + \frac{\beta}{n} + \frac{\beta\delta}{4}, \\ \|\dot{\bar{F}}^{(kl)}\|_\infty < \beta + \frac{2\beta}{n\delta}, \end{cases} \quad (16)$$

where $\bar{F}^{(kl)}(\lambda)$ is spanned by the standard orthonormal basis $\{1, \lambda, \dots, \lambda^{n-1}\}$ and $\delta = 2\sqrt{\delta/n}$ [13]. Note that for any $(p+q) \times q$ -dimensional complex matrix $X(e^{j\omega})$, one has that^[17]

$$\bar{\sigma}(X(e^{j\omega})) \leq \sqrt{q(p+q)} \max_{\substack{k \in \mathcal{K} \\ l \in \mathcal{L}}} |X^{(kl)}(e^{j\omega})|, \quad \forall \omega \in \mathcal{T}. \quad (17)$$

According to (16) and (17), the associated conclusion of this theorem can be derived.

During the quantification of the worst-case error e_{wc} , the coprimeness between $\bar{N}_F(\lambda)$ and $\bar{D}_F(\lambda)$ is also needed to be satisfied and this condition can resort to the following lemma.

Lemma 3 If the following inequality holds

$$n > \frac{\beta}{\frac{\rho_1}{q} - \alpha}, \quad (18)$$

then $\bar{N}_F(\lambda)$ and $\bar{D}_F(\lambda)$ are coprime.

Proof Taking the limit of $\bar{\delta} \rightarrow 0$ to the first inequality in (13) gives rise to

$$\bar{\sigma}(D_m(e^{j\omega}) - \bar{D}_F(e^{j\omega})) \leq q\left(\alpha + \frac{\beta}{n}\right), \quad \forall \omega \in \mathcal{T}. \quad (19)$$

If the right hand side of the above inequality is further strictly less than ρ_1 for any $\omega \in \mathcal{T}$, i.e.,

$$q\left(\alpha + \frac{\beta}{n}\right) < \rho_1, \quad (20)$$

then $\text{wno}[\det(\bar{D}_F)] = \text{wno}[\det(D_m)]$ can be derived according to fact in [18]. Since $D_m(e^{j\omega})$ for $\omega \in \mathcal{T}$ can be similarly constructed in terms of (9) and thus is a real-value matrix, $\text{wno}[\det(D_m)] = 0$ can be readily obtained. As a result, one has $\text{wno}[\det(\bar{D}_F)] = 0$. Further note that $\bar{D}_F(\lambda)$ belongs to $\mathbb{H}_\infty^{q \times q}$, it can be concluded that $\bar{D}_F^{-1}(\lambda)$ also belongs to $\mathbb{H}_\infty^{q \times q}$ and thus the coprimeness between $\bar{N}_F(\lambda)$ and $\bar{D}_F(\lambda)$ is ensured. Therefore, the constraint condition in this lemma is directly derived from (20).

Besides, the existence of $\delta_v(P_m, \bar{N}_F \bar{D}_F^{-1})$ is also needed. Since $\bar{D}_F(\lambda)$ is a unit function in $\mathbb{H}_\infty^{p \times p}$ under the condition (20), a sufficient condition for the existence of $\delta_v(P_m, \bar{N}_F \bar{D}_F^{-1})$ can be given as follows according to Lemma 1

$$\bar{\sigma}(\tilde{G}_m \bar{G})(e^{j\omega}) < \rho_1, \quad \forall \omega \in \mathcal{T}, \quad (21)$$

where $\bar{G}(\lambda)$ is a NRGS of $\bar{N}_F(\lambda) \bar{D}_F^{-1}(\lambda)$. This constraint condition can be ensured as long as a sufficient-

ly large n is taken. In this case, the following point-wise chordal distance at any $\omega_i \in \mathcal{W}$ can be bounded (c.f. [13])

$$\begin{aligned} \kappa(P_m, \bar{N}_F \bar{D}_F^{-1})(e^{j\omega_i}) &= \\ \bar{\sigma}(G_m - \bar{F} \bar{Q}_F)(e^{j\omega_i}) &\leq \\ \bar{\sigma}(G_m - \bar{F})(e^{j\omega_i}) &\leq \\ \sqrt{q(p+q)}\left(\alpha + \frac{\beta}{n} + \frac{\beta\delta}{4}\right), \end{aligned} \quad (22)$$

where $\bar{Q}_F(e^{j\omega_i}) = [(\bar{F}^* \bar{F})(e^{j\omega_i})]^{-1}(\bar{F}^* G_m)(e^{j\omega_i})$.

In order to quantify the worst-case error e_{wc} , we start from bounding the minimization objective function in (8). Suppose that the possible optimal solutions are \hat{X} and $\hat{Q}_F^{\omega_i}$ and the corresponding optimal objective function value is γ_{opt} . As a consequence, one has that

$$\gamma_{opt} = \max_{\omega_i \in \mathcal{W}} \left\{ \max_{\hat{X}} \left\{ \bar{\sigma}(G_m^{\omega_i} - F_{\hat{X}}^{\omega_i} \hat{Q}_F^{\omega_i}) \right\}, \tilde{c}(\bar{\delta})^r \|\hat{F}_{\hat{X}}\|_{\infty} \right\} \quad (23)$$

whose upper bound can be determined as

$$\begin{aligned} \gamma_{opt} < \gamma_b \triangleq \\ \max \left\{ \sqrt{q(p+q)}\left(\alpha + \frac{\beta}{n} + \frac{\beta}{2} \sqrt{\frac{\bar{\delta}}{n}}\right), \right. \\ \left. \sqrt{q(p+q)}\tilde{c}(\bar{\delta})^r \left(\beta + \frac{\beta}{\sqrt{\bar{\delta}n}}\right) \right\}, \end{aligned} \quad (24)$$

which results from Theorem 1 and (22).

According to the similar derivation process in [13], for any $\omega^* \in \mathcal{T}$, the chordal distance between $P_0(e^{j\omega})$ and $\hat{P}(e^{j\omega})$ can be quantified as

$$\begin{aligned} \kappa(P_0, \hat{P})(e^{j\omega^*}) < \\ \|\hat{G}_0\|_{\infty} \frac{\bar{\delta}}{2} + \bar{\sigma}(G_0(e^{j\omega_i}) - G_m(e^{j\omega_i})) + \\ \gamma_b + \|\hat{F}_{\hat{X}}\|_{\infty} \frac{\bar{\delta}h}{2}. \end{aligned} \quad (25)$$

According to (5)(12) and (13), the upper bound for the worst-case error e_{wc} can be eventually determined as

$$\begin{aligned} e_{wc} < \alpha + \gamma_b + \frac{\bar{\delta}\beta}{2} \left[1 + \right. \\ \left. h\sqrt{q(p+q)}\left(1 + \frac{1}{\sqrt{\bar{\delta}n}}\right) \right] \triangleq \tau. \end{aligned} \quad (26)$$

Remark 1 In order to further reduce the conservativeness of the resulting worst-case error bound, we employ the second inequality in (13) instead of (24), which is used as an inequality for the quantification of the worst-case error in [13].

3.2 Convergent theorem

With the expression of the worst-case error bound τ defined in (26), the following robust convergent theorem for the optimization algorithm resulting from (8) can be obtained.

Theorem 2 If \hat{X} and $\hat{Q}_F^{\omega_i}$ are the optimal solutions of (8) via the two-step iterative procedure in

[13–14] provided that the Nyquist winding condition $\text{wno}[\det(G_m^* F)] = 0$ as well as the constraints (18) and (21) holds, then one has

$$\begin{aligned} \lim_{\bar{\delta} \rightarrow 0} \lim_{\epsilon \rightarrow 0} e_{wc}(\beta, \epsilon, n, p, q, \bar{\delta}, \tilde{c}, r, h) < \\ e_1(\beta, n, p, q) = \frac{\beta}{n} \sqrt{q(p+q)} \end{aligned} \quad (27)$$

and

$$\begin{aligned} \lim_{n \rightarrow \infty} \lim_{\epsilon \rightarrow 0} e_{wc}(\beta, \epsilon, n, p, q, \bar{\delta}, \tilde{c}, r, h) < \\ e_2(\beta, p, q, \bar{\delta}, \tilde{c}, r, h) = \\ \frac{\bar{\delta}\beta}{2} + \beta \sqrt{q(p+q)} [\tilde{c}(\bar{\delta})^r + \frac{\bar{\delta}h}{2}] \end{aligned} \quad (28)$$

with

$$\begin{aligned} \lim_{n \rightarrow \infty} e_1(\beta, n, p, q) &= 0, \\ \lim_{\bar{\delta} \rightarrow 0} e_2(\beta, p, q, \bar{\delta}, \tilde{c}, r, h) &= 0. \end{aligned}$$

Proof This theorem can be directly derived from (26) by taking the corresponding limits into consideration.

From this theorem, it can be concluded that the optimization algorithm from (8) is robust convergent under some specified conditions and thus can be applicable to the worst-case identification of the MIMO EIV models.

4 Algorithm implementation

This section will address the implementation issues for the optimization algorithm originating from (8).

4.1 Constraint consideration

For an application of the optimization criterion in (8), the coprimeness between $N_F^X(\lambda)$ and $D_F^X(\lambda)$ should be ensured in advance, whose sufficient condition can be stated as

$$n > \frac{\beta}{\frac{\rho_1}{q} - \alpha}, \quad (29)$$

which is the same as (18) in Lemma 3 and thus can be derived similarly. Under the above condition, $D_F^X(\lambda)$ is definitely a unit function in $H_{\infty}^{q \times q}$. In addition, the associated Nyquist winding condition $\text{wno}[\det(G_m^* F)] = 0$ for the former objective function in (8) should be also satisfied. According to Lemma 1, this condition can be guaranteed provided $D_F^X(\lambda)$ is a unit function. Fortunately, the latter condition can also be ensured by (29) and thus it is necessary to satisfy the following precondition

$$\bar{\sigma}(\tilde{G}_m G)(e^{j\omega}) < \rho_1, \quad \forall \omega \in \mathcal{T}, \quad (30)$$

which is given by Lemma 1. The quantity in the left hand side of (30) is equal to the former objective function in (8) when both are evaluated at $\omega_i \in \mathcal{W}$ and thus it is conveniently constrained in the associated algorithm implementation.

In a matter of fact, in the quantification of the worst-

case error using the v-gap metric, the following sufficient conditions should be satisfied, i.e.,

$$\delta_v(P_m, \hat{P}) < \rho_1, \quad (31)$$

$$\delta_v(\hat{P}, P_0) < \tau < \inf_{\omega \in \mathcal{T}} \bar{\sigma}(\hat{D}(e^{j\omega})) \triangleq \rho_2, \quad (32)$$

where $\hat{D}(e^{j\omega})$ is the frequency response of the denominator factor of a NRGS of $\hat{P}(\lambda)$. While (31) is implied by Lemma 1, (32) is used to ensure the applicability of the worst-case error bound τ . These two constraints are related to the noises (n_y, n_u) and thus the complementary noise set in (11) is defined as

$$\mathcal{S}_{N_2}(\rho_1, \rho_2) \triangleq \{(n_y, n_u) : \delta_v(P_m, \hat{P}) < \rho_1 \text{ and } \delta_v(\hat{P}, P_0) < \tau < \rho_2\}. \quad (33)$$

In addition, the upper bound h for $\|Q_F\|_\infty$ should be known, which can be bounded in the following way. One first obtains that

$$\begin{aligned} \bar{\sigma}[\hat{Q}_F(e^{j\omega})] &= \\ \bar{\sigma}\{[(F_X^* F_X)(e^{j\omega})]^{-1} (F_X^* G_m)(e^{j\omega})\} &\leq \\ \frac{\bar{\sigma}[F_X(e^{j\omega})]}{2\sigma[F_X(e^{j\omega})]}. \end{aligned} \quad (34)$$

By taking a super operation to the above inequality for $\omega \in \mathcal{T}$, h can be determined as

$$h \triangleq \sup_{\omega \in \mathcal{T}} \frac{\bar{\sigma}[F_X(e^{j\omega})]}{2\sigma[F_X(e^{j\omega})]}. \quad (35)$$

It should be noted that the optimization of (8) can be recursively solved by two interactively iterated minimization problems as in [13–14]. However, the computation of $c\|\hat{F}_X\|_\infty < \gamma$ in the MIMO case has a little difference from that in the SISO case. In the former case, we should manage to make a state-space realization $\{A, B, C, D\}$ for \hat{F}_X be minimal and thus the resulting computational efficiency will be inevitably improved to some extent. Meanwhile, we should also make the parameters to be optimized exist in C and D so that such realization can form a linear matrix inequality constraint.

4.2 Identification steps

The identification procedure for identification of a MIMO EIV model can be summarized as follows.

Step 1 Determine the a priori model set $\mathcal{S}_{\mathcal{M}}(\beta)$ and the a priori noise set $\mathcal{S}_{N_1}(\epsilon)$ by various pre-experiments.

Step 2 Generate $G_m^{\omega_i}$, $\omega_i \in \mathcal{W}$ using the frequency-domain data $\mathcal{S}_{\mathcal{D}}(\mathcal{W})$ from identification experiments according to (9).

Step 3 Parameterize $F_X(\lambda)$ in terms of (10).

Step 4 Obtain $\hat{P}(\lambda)$ via the optimization of the minimization problem (8).

Step 5 Quantify a worst-case error bound τ for $\hat{P}(\lambda)$ in accordance with (26).

Remark 2 The identified nominal system model $\hat{P}(\lambda)$ and the quantified worst-case error bound τ are able to characterize a robust control-oriented model set, which paves the way for the robust controller design using H_∞ loop-shaping synthesis methods via v-gap metric [15].

5 Simulation

The MIMO EIV model identification procedure is verified on the following double-input and single-output system

$$P_0(\lambda) = \begin{bmatrix} \lambda + \frac{1}{9} & \lambda + \frac{1}{8} \\ \lambda + \frac{1}{9} & \lambda + \frac{1}{8} \end{bmatrix}, \quad (36)$$

whose frequency responses are corrupted by the corresponding zero-mean Gaussian white noises with the following sampling angular frequency dependent variances

$$\begin{cases} \sigma_1^2(\omega_i) = \frac{e^{j\omega_i} + \frac{1}{9}}{e^{j\omega_i} + \frac{1}{2}}, \\ \sigma_2^2(\omega_i) = \frac{e^{j\omega_i} + \frac{1}{8}}{e^{j\omega_i} + \frac{1}{8}}, \end{cases} \quad \omega_i \in \mathcal{W}, \quad (37)$$

which derive from (36) in a straightforward manner.

In the above simulation environment, ρ_0 and β can be determined as 0.9622 and 0.3755, respectively. The a priori noise bound can be calculated as $\epsilon = 0.0718$, which is less than ρ_0 . The corrupted frequency responses with the data length $N = 40$ are uniformly collected from the sampling frequency interval $[0.001, \pi - 0.001]$ and thus $\bar{\delta}$ can be computed as 0.0805. ρ_1 is approximated as $\min_{\omega_i \in \mathcal{W}} D_m(e^{j\omega_i}) = 0.9477$. In the model parametrization in (10), $n = 4$ is selected such that (29) is satisfied. During the optimization of (8), the choice for c is made as

$$\tilde{c} = 1, \quad r = 0.8. \quad (38)$$

After the implementation of the proposed identification procedure, the optimal parameters for the numerator and denominator factors are

$$\begin{aligned} X_N &= \\ &[0.0030, 0.2112, -0.0365, -0.0015, \\ &0.0226, 0.1099, -0.0196, 0.0100], \\ X_D(1, :) &= \\ &[0.9750, 0.0041, 0.0020, 0.0010, \\ &-0.0205, 0.0024, -0.0019, -0.0124], \\ X_D(2, :) &= \\ &[0.0005, 0.0000, -0.0000, 0.0004, \\ &0.9938, -0.0002, 0.0008, -0.0010], \end{aligned}$$

where $X_D(l, :)$ means all the elements in the l th row. Meanwhile, the corresponding optimal value is ob-

tained as 0.0736. The identified transfer functions in $P_0(\lambda)$ are compared with their respective true models in Figs.2 and 3, respectively. We can also compute the worst-case error bound as $\tau = 0.6615$ accordingly. Therefore, the identified nominal system model $\hat{P}(\lambda)$ and τ characterize a model set which contains the true system $P_0(\lambda)$ and this model set paves the way for its later robust controller synthesis.

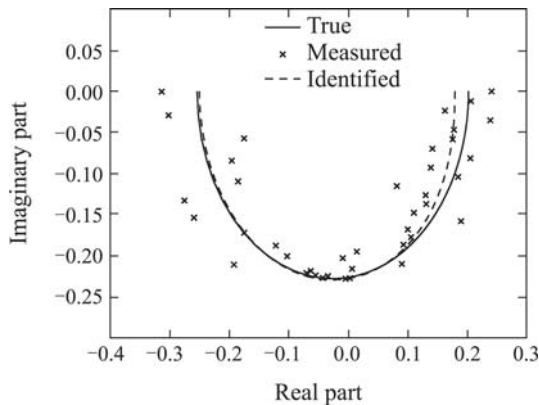


Fig. 2 Identification of the 1st transfer function in $P_0(\lambda)$

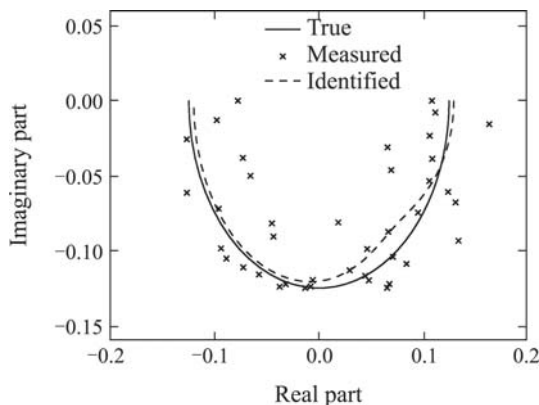


Fig. 3 Identification of the 2nd transfer function in $P_0(\lambda)$

It can be shown from these two figures that the resulting identification results are satisfactory and the effectiveness of the proposed method has thus been verified.

6 Conclusion

A frequency-domain worst-case identification method for MIMO EIV models is proposed in this paper to cater for the robust control design. This identification method is an extension to that for the SISO case. The relevant identification framework for the MIMO EIV models is clarified and then the corresponding identification algorithm is addressed for the estimation of a nominal system model. We put an emphasis on the quantification of a worst-case error for the estimated nominal system model and a proof of the robust convergent theorem for the proposed algorithm. A simulation example is given to show the effectiveness of the proposed identification method.

References:

- [1] LJUNG L. *System Identification: Theory for the User* [M]. Upper Saddle River, NJ: Prentice Hall PTR, 1999.
- [2] LJUNG L, SÖDERSTRÖM T. *Theory and Practice of Recursive Identification* [M]. London: the MIT Press, 1983.
- [3] SÖDERSTRÖM T. A generalised instrumental variable estimator for multivariable errors-in-variables identification problems [J]. *International Journal of Control*, 2012, 85(3): 287 – 303.
- [4] CHEN H. Recursive identification for multivariate errors-in-variables systems [J]. *Automatica*, 2007, 43(7): 1234 – 1242.
- [5] DIVERSI R, GUIDORZI R. Combining the Frisch scheme and Yule-Walker equations for identifying multivariable errors-in-variables models [C] // *Proceedings of the 19th International Symposium on Mathematical Theory of Networks and Systems*. Budapest, Hungary, July: [s.n.], 2010: 2407 – 2413.
- [6] DIVERSI R, GUIDORZI R. Frisch scheme-based identification of multivariable errors-in-variables models [C] // *Proceedings of the 15th IFAC Symposium on System Identification*. St. Malo, France: [s.n.], 2009: 1563 – 1567.
- [7] STANKOVIĆ M S, STANKOVIĆ S S, STIPANOVIĆ D M. Decentralized identification for errors-in-variables systems based on a consensus algorithm [C] // *Proceedings of the 50th IEEE Conference on Decision and Control and European Control Conference*. Orlando, FL: IEEE, 2013, 413(1): 2951 – 2956.
- [8] CHOU C T, VERHAEGEN M. Subspace algorithm for the identification of multivariable dynamic errors-in-variables models [J]. *Automatica*, 1997, 33(10): 1857 – 1869.
- [9] GREEN M, ANDERSON B. Identification of multivariable errors-in-variables models with dynamics [J]. *IEEE Transactions on Automatic Control*, 1986, 31(5): 467 – 471.
- [10] ROORDA B, HEIJ C. Global total least squares modeling of multivariable time series [J]. *IEEE Transactions on Automatic Control*, 1995, 40(1): 50 – 63.
- [11] GENG L H, GENG L Y, LU S L, et al. L_2 -optimal identification of MIMO errors-in-variables models from the v-gap geometrical interpretation [J]. *International Journal of Control*, 2012, 85(7): 898 – 905.
- [12] GENG L H, GENG L Y. L_2 -optimal identification of MIMO errors-in-variables models [C] // *Proceedings of the International Conference on Electrical and Control Engineering*. Yichang, China: IEEE, 2011: 4548 – 4551.
- [13] GENG L H, XIAO D Y, ZHANG T, et al. Robust control oriented identification of errors-in-variables models based on normalised coprime factors [J]. *International Journal of Systems Science*, 2012, 43(9): 1741 – 1752.
- [14] DATE P, VINNICOMBE G. Algorithms for worst-case identification in H_∞ and in the v-gap metric [J]. *Automatica*, 2004, 40(6): 995 – 1002.
- [15] VINNICOMBE G. *Uncertainty and Feedback: H_∞ Loop-Shaping and the V-gap Metric* [M]. London: Imperial College Press, 2000.
- [16] GENG L H, CUI S G, XIA Z Y. Error quantification of the normalised right graph symbol for an errors-in-variables system [J]. *Control Theory and Technology*, 2015, 13(3): 238 – 244.
- [17] AKÇAY H, NINNESS B. Rational basis functions for robust identification from frequency and time-domain measurements [J]. *Automatica*, 1998, 34(9): 1101 – 1117.
- [18] VINNICOMBE G. Frequency domain uncertainty and the graph topology [J]. *IEEE Transactions on Automatic Control*, 1993, 38(9): 1371 – 1383.

作者简介:

耿立辉 (1977–), 男, 副教授, 硕士生导师, 目前研究方向为系统辨识及状态估计, E-mail: glh2010@tute.edu.cn;

崔世钢 (1963–), 男, 教授, 博士生导师, 目前研究方向为机器人运动控制, E-mail: csg@163.com;

赵丽 (1962–), 女, 教授, 博士生导师, 目前研究方向为现代信号处理, E-mail: jinshihui@163.com.